

Two Modes of Solid State Nucleation — Ferrites, Martensites and Isothermal Transformation Curves

Madan Rao* and Surajit Sengupta†

*Raman Research Institute, C.V. Raman Avenue, Bangalore 560080, India

†S. N. Bose National Centre for Basic Sciences, Block JD, Sector III, Salt Lake, Calcutta 700091, India

(June 6, 2024)

When a crystalline solid such as iron is cooled across a structural transition, its final microstructure depends sensitively on the cooling rate [1,2]. For instance, an adiabatic cooling across the transition results in an equilibrium ‘ferrite’, while a rapid cooling gives rise to a metastable twinned ‘martensite’ [2]. There exists no theoretical framework to understand the dynamics and conditions under which both these microstructures obtain. Existing theories of martensite dynamics [3–6] describe this transformation in terms of elastic strain, without any explanation for the occurrence of the ferrite. Here we provide evidence for the crucial role played by non-elastic variables, *viz.*, dynamically generated interfacial defects. A molecular dynamics (MD) simulation of a model 2-dimensional (2d) solid-state transformation reveals two distinct modes of nucleation depending on the temperature of quench. At high temperatures, defects generated at the nucleation front relax quickly giving rise to an isotropically growing ‘ferrite’. At low temperatures, the defects relax extremely slowly, forcing a coordinated motion of atoms along specific directions. This results in a twinned critical nucleus which grows rapidly at speeds comparable to that of sound. Based on our MD results, we propose a solid-state nucleation theory involving the elastic strain and non-elastic defects [7,8], which successfully describes the transformation to both a ferrite and a martensite. Our work provides useful insights on how to formulate a general dynamics of solid state transformations.

We study a 2d model system which exhibits exactly two distinct equilibrium solid phases — a square and a triangular phase (with a rhombic unit cell) using an MD simulation on particles (‘atoms’) interacting with an effective 2- and 3-body potential (see Fig. 1). By tuning the potential parameters, we induce a square-to-triangular solid-state transformation at constant temperature. Figure 1 shows two typical ‘quenches’ (referred to as high temperature T_1 and low temperature T_2 quenches) starting from the equilibrium square phase. In both cases following the quench, the product phase is formed by a process of nucleation and growth (Fig. 1 (inset)), but while the T_1 nucleation is homogeneous, the T_2 nucleation needs to be seeded by a single defect (heterogeneous). Nucleation of a triangular region within the square phase

gives rise to vacancies/interstitials due to atomic mismatch, which relax with a temperature dependent diffusion coefficient [1]. Note that (a) the use of effective potentials rather than ‘realistic’ atomic potentials allows us to probe late times and large sizes; (b) the experimentally more accurate quench schedule is a cut through the $T-v_3$ plane, however the essential physics is unaltered by our constant T quench allowing for a more transparent interpretation of the MD results.

In an earlier paper [9], we had presented a coarse-graining procedure which starts from a microscopic description of a solid and constructs continuum variables relevant for a description of the solid at larger length scales. Thus we define coarse-grained dynamical *elastic* variables from the instantaneous displacements \mathbf{u} of the particles from the ideal square lattice [9] — nonlinear strain $\epsilon_{ij} = 1/2(\partial_i u_j + \partial_j u_i + \partial_i u_l \partial_j u_l)$, density fluctuation about the mean $\langle \rho \rangle$, $\phi = (\rho - \langle \rho \rangle) / \langle \rho \rangle$ (we shall refer to this as the vacancy/interstitial field) and dislocation density (density of 5-7 disclination pairs).

In the T_1 quench the vacancies/interstitials diffuse fast and annihilate each other, thus encouraging the triangular phase to grow isotropically (Fig. 2a) with a size R that grows linearly with time t . The critical nucleus is untwinned leading to a polycrystalline triangular solid (‘ferrite’).

In the T_2 quench the seed vacancy does not diffuse away; dominant fluctuations correspond to a coordinated movement of a line segment of atoms along the square axes (Fig. 3a). Once these fluctuations get large enough, they grow into a twinned critical nucleus with the twinning plane along one of the square axes. The twinned nucleus grows anisotropically, with a constant tip speed roughly equal to that of longitudinal sound (Fig. 3b). The vacancies and interstitials while staying separated from each other, are found concentrated at the interface of the growing nucleus (Figs. 3c). In the direction transverse to the twinning ‘plane’, the nucleus grows by step formation (Fig. 3a).

The MD simulation highlights the crucial role played by defects in determining the mode of nucleation and the nature of the critical nucleus. From these simulations we learn that the relevant variables to describe the dynamics of nucleation should include *both* the strain ϵ_{ij} [10] and the defect density ϕ . We now describe an analytic theory of solid-state nucleation for which the simplest dimensionless free-energy functional describing the first-order square ($\langle \epsilon_{xy} \rangle = 0$) to rhombus ($\langle \epsilon_{xy} \rangle = \pm e_0$)

transition at a fixed degree of undercooling a has the form,

$$F = \int_{x,y} (\nabla w_{ij})^2 + a\epsilon_{xy}^2 + b\epsilon_{ii}^2 - \epsilon_{xy}^4 + \epsilon_{xy}^6 + \gamma\phi^2 + C\phi\epsilon_{ii} \quad (1)$$

where $w_{ij} \equiv \partial_i u_j$ is the deformation tensor. A quench across this transition to where the square phase is metastable, nucleates a small ‘droplet’ of the rhombus. Following the MD, we simultaneously create an envelope of ϕ around the droplet; this is the initial condition for the dynamical equations in the displacements \mathbf{u} [7,11] and ϕ : $\partial_t \phi + \mathbf{v} \cdot \nabla \phi = D_v \nabla^2 (2\gamma\phi + C\epsilon_{ii})$, where the microscopic vacancy diffusion coefficient has an Arrhenius form $D_v = D_\infty \exp(-A/k_B T)$, with an activation energy A [1]. The velocity field $\mathbf{v} = \dot{\mathbf{u}} + \Gamma C \nabla \phi$, where Γ is the microscopic kinetic coefficient of \mathbf{u} .

For a high temperature quench D_v is large, so ϕ relaxes much faster than the time for the critical nucleus to form; subsequently the nucleus grows isotropically into an equilibrium triangular solid (‘ferrite’) [7,8] with $R \sim t$.

For intermediate temperature quenches D_v is smaller; the nature of the critical nucleus is determined by computing the time taken for critical nucleation τ_n (‘first-passage-time’). Apriori we do not know whether the critical nucleus is twinned or not, and so we perform a variational calculation for both cases; the ‘true critical nucleus’ is the one for which τ_n is smaller.

In the linearised equation for ϕ , the velocity field (ignoring lattice vibrations) reduces to the front velocity $\mathbf{v} = v_f \hat{\mathbf{n}} \delta(\mathbf{r} - \mathbf{R}(t))$, where $\mathbf{R}(t)$ is the position of the moving interface and $\hat{\mathbf{n}}$ is the unit outward normal to the interface. Thus in the reference frame of the interface, the dynamics of ϕ is diffusive. Since the relaxation time to the local minima of Eq. (1) is smaller than barrier hopping times, we may treat ϵ_{ij} as ‘slaved’ to ϕ in the calculation of the barrier height [12]. We then use a Kramers’ formula to evaluate τ_n , thus apart from unknown prefactors, $\tau_n = \Gamma^{-1} \exp(\Delta E^*/k_B T)$, where ΔE^* is the $\phi(\mathbf{r}, t)$ -dependent critical barrier energy. Figure 4 clearly shows that for high temperature quenches (low undercooling), the true critical nucleus is a ‘ferrite’, while for a low temperature quench it forms a twinned bicrystal. We successfully reproduce two distinctive features of the well known 0% isothermal transformation curves of martensites — the horizontal transformation curve beyond a well defined ‘start’ temperature M_s independent of D_∞ , and a ferrite nose. It should be remarked that such a calculation could not even be addressed within the conventional viewpoint.

What happens after the twinned critical nucleus is formed? It is difficult to say based on our early time MD studies, whether the growing nucleus will eventually add on more twins or whether it will continue as a bicrystal with a single twin interface. On the other hand we may analyse the late time dynamics within our

analytic formalism. In the limit $D_v \rightarrow 0$ when ϕ remains frozen at the moving interface, a constrained variational calculation [7,8], shows that the growing nucleus finds it favourable to add more twins. The free energy of an anisotropic inclusion of length L and width W , with N twins along the length is given by $F = \Delta F L W + \sigma_{pp}(L + W) + \sigma_{tw} N W + \beta(L/N)^2 N$, where $\Delta F < 0$ is the free energy difference between the square and triangular phases, σ_{pp} and σ_{tw} are the surface tensions of the square-rhombus and the twin interfaces respectively, and the last term is the ϕ contribution at the square-rhombus interface. Minimization with respect to N gives $L/N \sim W^{1/2}$, a relation that is empirically known for 2d martensites like In-Tl [2,10]. Moreover the energy of the nucleus is smaller when oriented along specific directions, the habit ‘planes’ [8].

The square-rhombus interface is studded with an array of vacancies such that $\phi \rightarrow 0$ on an average, with a separation equal to the twin size. Thus the strain decays exponentially from the interface over a distance of order L/N . This ‘fringing field’ [10] arises dynamically in our calculation, rather than from an imposed boundary condition [10]. Indeed throughout our analysis we do not impose specific interfacial conditions [6,10], preferring to allow the solid to choose its own dynamical path.

The theoretical formalism just presented may be generalised to arbitrary solid-state transformations. We have found that in order to develop a general theory for solid state nucleation, it is necessary to go beyond nonlinear elasticity theory. More specifically, *the complete set of relevant dynamical variables should include non-elastic degrees of freedom* like defect fields. Such non-elastic degrees of freedom should be relevant whenever a solid undergoes large shear deformations. Our work provides a framework to understand the dynamics of solid state transformations and the conditions under which various microstructures obtain. The methodology of translating from microscopic simulations to coarse-grained dynamical fields should be useful in other problems in material science such as brittle-ductile transitions. We are currently generalising our theory to include the dynamics of dislocations, substitutional and interstitial impurities and a coupling to external stress to study the dynamics of shape-memory alloys.

-
- [1] Cahn, R. W. and Haasen, P. *Physical Metallurgy* (North-Holland, Amsterdam, 1996).
 - [2] Nishiyama, Z. *Martensitic Transformation* (Academic Press, NY, 1978).
 - [3] Kachaturyan, A. G. *Theory of Structural Transformations in Solids* (Wiley, NY, 1983).

- [4] Bales, G. S. and Gooding, R. J. *Interfacial dynamics at a first-order phase transition involving strain: dynamical twin formation*. Phys. Rev. Lett. **67**, 3412-3415 (1991).
- [5] Reid, A. C. E. and Gooding, R. J. *Hydrodynamic description of elastic solids with open boundary conditions undergoing a phase transition*. Phys. Rev. B **50**, 3588-3602 (1994).
- [6] van Zyl, B. P. and Gooding, R. J. *A comprehensive dynamical study of nucleation and growth at a 1D shear martensite transformation*. Met. Trans. A **27**, 203 (1996).
- [7] Rao, M. and Sengupta, S. *Droplet fluctuations in the morphology and kinetics of martensites*. Phys. Rev. Lett. **78**, 2168-2171 (1997).
- [8] Rao, M. and Sengupta, S. *Arrested states in solids*. Curr. Sc. **77**, 382-387 (1999).
- [9] Sengupta, S., Nielaba, P., Rao, M. and Binder, K. *Elastic constants from microscopic strain fluctuations*. Phys. Rev. E **61**, 1072-1080 (2000).
- [10] Barsch, G. R., Horovitz, B. and Krumhansl, J. A. *Dynamics of twin boundaries in martensites*. Phys. Rev. Lett. **59**, 1251-1254 (1987).
- [11] Martin, P. C., Parodi, O. and Pershan, P. S. *Unified hydrodynamic theory for crystals, liquid crystals and normal fluids*. Phys. Rev. A **6**, 2401-2420 (1972).
- [12] Rao, M. and Sengupta, S. *First passage times and time-temperature-transformation curves for martensites*. lanl eprint: cond-mat/9709022.

Acknowledgements We are grateful to S. Mayor and S. Sastry for a careful reading of the manuscript. We thank the participants of the 1999 workshop on ‘Mathematical methods in solid mechanics and material science’ at the Isaac Newton Institute, Cambridge, for several illuminating discussions. MR thanks the Department of Science and Technology, India for the award of a Swarnajayanthi fellowship.

Correspondence and requests for materials should be addressed to M. R. (e-mail: madan@rri.ernet.in)

Figure Caption

Fig. 1 **Phase diagram in the $T - v_3$ plane** at a density $\langle\rho\rangle = 1.05$ using an MD simulation in the NVT ensemble. The particles interact via an effective potential consisting of a 2-body $V_2(r_{ij}) = v_2(\sigma/r_{ij})^{12}$ and a short range 3-body $V_3(\mathbf{r}_i, \mathbf{r}_j, \mathbf{r}_k) = v_3[\sin^2(4\theta_{ijk}) + \sin^2(4\theta_{jki}) + \sin^2(4\theta_{kij})]$. Particles i and j are separated by a distance r_{ij} . θ_{ijk} is the bond angle at j between triplets (ijk) . V_2 favours a triangular lattice ground state while V_3 is minimised when $\theta_{ijk} = 0, \pi/4, \pi/2$ and so favours a square lattice. The units of length and energy are set by σ and v_2 respectively, making the unit of time $\sigma\sqrt{m/v_2}$, where m is the particle mass. The MD time step is 0.001 corresponding roughly to a real time of 1 fs. The order parameter $\langle\Omega\rangle = (\Omega_0 N)^{-1} \sum_{ijk} \langle\sin^2(4\theta_{ijk})\rangle$ takes values 0(1) in the square(triangular) phases respectively. The phase diagram was obtained by equilibrating a system of $N = 1024$ particles at various values of T and v_3 . Arrows marked T_1 and T_2 are constant temperature quenches at $T_1 = 1$ and $T_2 = 0.15$. The values of v_3 to which the solid is quenched is $v_3 = 3$ and $v_3 = 1.2$ respectively, which lie in the region of the phase diagram where the square is metastable (within the dotted line). Inset shows the time evolution of $\langle\Omega\rangle$ for the two quenches, T_1 (thin line) and T_2 (thick line), indicating a typical nucleation process.

Fig. 2 **MD snapshot at $t = 10^4$ following a T_1 quench:** ‘Ferrite’ nucleus grows isotropically as a polycrystalline triangular region. The colours code the local values of $\langle\Omega\rangle$ going from red in the square region to blue in the triangular region. Inset shows x-y trajectories for $5 \times 10^3 < t < 25 \times 10^3$ of 5 particles chosen to lie along a row (x -axis) at $t = 0$. At these times the particles are part of the growing nucleus, and their trajectories reveal significant diffusive motion. Number of unit cells of the square in each direction is 110. The vacancy/interstitial density ϕ relaxes fast and quickly averages to 0.

Fig. 3 **MD snapshot at $t = 6 \times 10^3$ following a T_2 quench:** (a) Twinned nucleus grows anisotropically. Colour coding as in Fig. 2. Inset shows trajectories for $10^3 < t < 16.5 \times 10^3$ of 5 particles chosen to lie along a row (x -axis) at $t = 0$ (movement from bottom to top of inset). At these times the particles are part of the growing nucleus, and their trajectories reveal highly co-ordinated, ‘military’ motion characteristic of martensites. Number of cells is the same as above. (b) Positions of 5 particles chosen to lie along a twin-column (y -axis) as a function of time. Apart from thermal oscillations, the particle positions change only when they encounter the moving front at $t = t_s$. A plot of the position of the i th particle y_i as a function of t_s gives the front-velocity $v_f = 9.7$. This compares well with the sound velocity calculated from the bulk modulus in the square phase. (c) The vacancy/interstitial density ϕ integrated over x as a function of y (along the twinning plane) at times $t_1 = 2000$ and $t_2 = 5000$. The arrow shows the direction of the displacement field resulting in an increased density

at one end of the nucleus and a reduced density at the other. Inset shows the shear strain ϵ_{xy} integrated over y showing the twin boundary at t_1, t_2 .

Fig. 4 **First-Passage-Times versus degree of undercooling** a for a twinned and untwinned critical nuclei. The calculation proceeds by recognising that a perfect triangular solid is obtained from a perfect square by the deformation, $R'_i = (\delta_{ij} + \epsilon_{ij})R_j$, involving a shear $\epsilon_{xy} = \epsilon_{yx} = \epsilon$ and volume compression $\epsilon_{xx} = \epsilon_{yy} = \epsilon^2/2$. We therefore parametrize ϵ_{ij} by the single function $\epsilon(\mathbf{r}, t)$. This admits a variational ansatz for (1) ‘ferrite’: $\epsilon = 0$ outside a grain of size L and $\epsilon = e_0$ inside, with a smooth interpolation of width ξ and (2) ‘twinned nucleus’: $\epsilon = 0$ outside a rectangular grain of length L , width W and $\epsilon = \pm e_0$ inside, connected by smooth interpolations. The diffusion equation, $\partial_t \phi = D_v \nabla^2 (2\gamma \phi + C \epsilon_{ii})$ is solved with the initial condition $\phi(\mathbf{r}, 0) = \Delta \mathbf{u} \cdot \hat{\mathbf{n}}$ ($\Delta \mathbf{u}$ is geometrical mismatch at the square-triangle interface and is proportional to the length of the interface). Note that $\Delta \mathbf{u} = 0$ at the twin interface. The free-energy of the grain at time t , $E(L, W, t; \{\xi_i\})$ is obtained from Eq. (1), which we minimize with respect to the widths $\{\xi_i\}$ for every L, W and t . The barrier energy ΔE^* and size L^*, W^* of the critical nucleus at every time t , is determined by the saddle-point. The energy of the critical nucleus decreases with time, and so a crude but easily calculable estimate of the first-passage-time is obtained by a self consistent solution of $\tau_n = \Gamma^{-1} \exp(\Delta E^*(\tau_n))$. The curves have been calculated for $D_\infty = 10^{14}$, $A = 7$, $\gamma = 0.2$ and $C = 0$. The upper dotted line represents the equilibrium transition temperature (zero undercooling). At small undercooling ϕ relaxes fast and the critical nucleus is a ‘ferrite’, the first-passage-time for which goes through a minimum. At larger undercooling, the single twin nucleates faster (bold line) than the untwinned grain (lower dotted line). The arrow shows the degree of undercooling M_s below which the twinned nucleus forms (‘martensite start’ temperature).

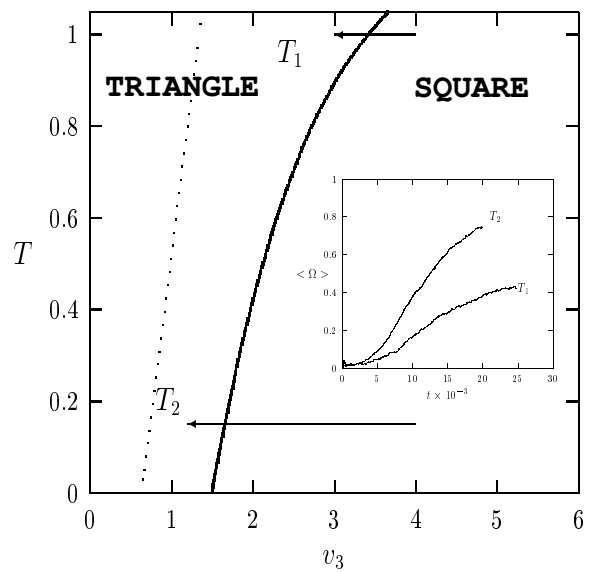


Fig. 1

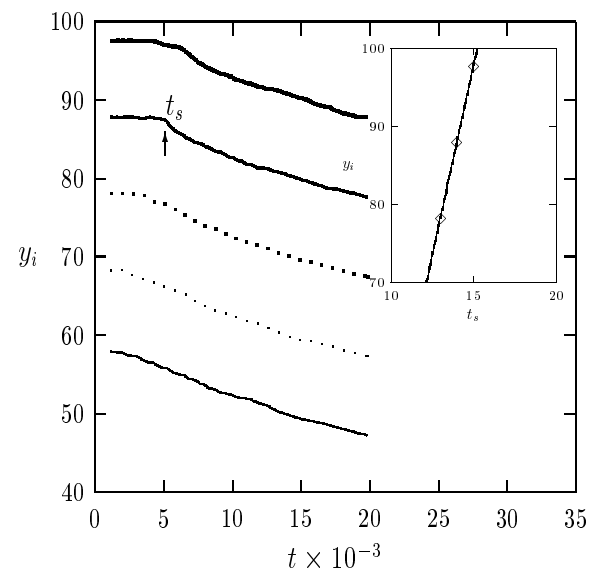


Fig. 3 (b)

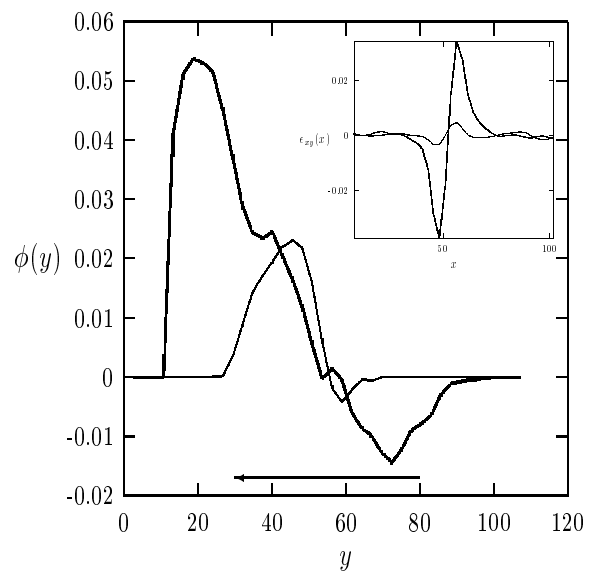


Fig. 3 (c)

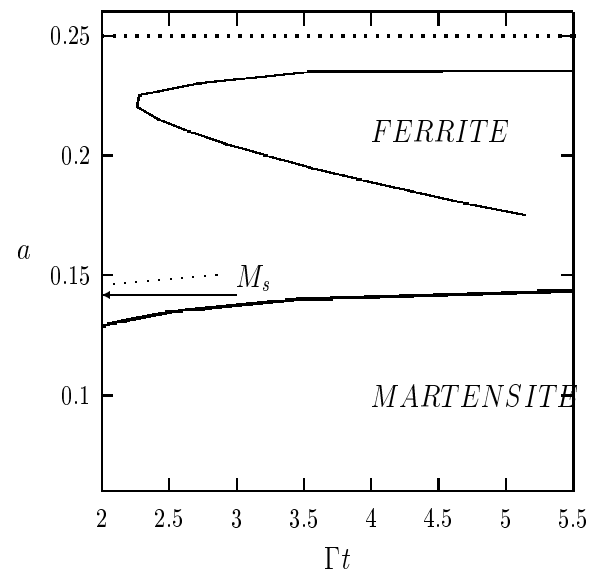


Fig. 4

This figure "color.jpg" is available in "jpg" format from:

<http://arxiv.org/ps/cond-mat/0107098v1>